

Dual Layer Structural Thermoplastic Polyester Powder Coating Film and Its Weathering Resistance

Yukitoshi Takeshita,¹ Takuya Kamisho,¹ Seizo Sakata,¹ Takashi Sawada,¹
Yoshikazu Watanuki,² Ryuichi Nishio,² Toshinobu Ueda²

¹NTT Energy and Environment Systems Laboratories, Nippon Telegraph & Telephone Corporation, 3-9-11, Midoricho, Musashino-shi, Tokyo 180-8585, Japan

²NTT Advanced Technology, 4-3-17 Shinkiba, Koto-ku, Tokyo 136-0082, Japan

Correspondence to: Y. Takeshita (E-mail: takeshita.yukitoshi@lab.ntt.co.jp)

ABSTRACT: Micro FTIR analysis was performed to the point with a 50–80 μm spatial resolution to verify the exact structure of a new blend thermoplastic powder coating film. Resistance to certain artificially accelerated conditions and actual outdoor exposure were examined to confirm the performance of the film as a protective coating for use in the telecommunication field. The new blend powder coating film consists of primary polyethylene terephthalate (PET) and secondary polyvinyl butyral (PVB) resins, and has a distinct dual phase structure. Specifically, it forms a continuous PVB phase in a surface layer with a thickness of approximately 100–150 μm . Good corrosion resistance was confirmed in artificially accelerated testing using salt water spray, heat cycle, and accelerated UV tests. Actual outdoor exposure in a metropolitan area (Shinkiba in Tokyo) and a coastal area (Miyake Island) revealed good weathering performance throughout the study period. © 2012 Wiley Periodicals, Inc. *J. Appl. Polym. Sci.* 000: 000–000, 2012

KEYWORDS: dual layer; powder coating; PET; PVB; corrosion resistance; weathering resistance

Received 21 April 2012; accepted 29 June 2012; published online

DOI: 10.1002/app.38299

INTRODUCTION

We provide telecommunication services throughout Japan, and this means that we have an enormous amount of telecommunication plant and material including approximately 2 million kilometers of cable, and nearly 12 million telephone poles.^{1,2} Outdoor plant materials in particular are exposed to a wide range of environments; UV light, a range of temperatures and humidity, sea salt particles, alkalinity, and acidity. Therefore, these materials are protected by some type of weathering prevention technology, and a wide variety of anti-corrosion technologies have been developed for each type of environment.^{3–6}

Polymeric materials such as those used for coatings offer highly effective protection and have been developed and introduced in the industrial telecommunication field. For instance, solvent-based coatings have been applied to wireless steel towers and cable pipes. Recently, environmentally friendly coatings, namely low solvent type and water-based coatings, have been in high demand, and they have been studied with a view to protecting human health and the environment.^{7–12}

Another example is steel telephone poles and their related steel supporting materials, which have a powder coating to increase

corrosion resistance and thus prevent damage caused by the natural environment.^{13–19} In particular, the bottom part of a steel telephone pole is exposed to more severe conditions than the rest of the pole. For instance, the bottom part of the pole comes into direct contact with the ground, mortar, and concrete, and therefore has the potential to be adversely affected by alkaline conditions. The literature includes many reports on the way that polymeric material is easily hydrolyzed in the presence of alkalinity.²⁰

Recently, we focused on improving the alkaline resistance of the conventional powder coatings developed in our laboratories, and tried to combine conventional powder resin with a highly alkaline resistant powder resin. In preliminary studies,^{21–23} we found by using Fourier transform infrared (FTIR) analysis that the first and second resins co-existed in the new blend coating films, and the surface region was dominated by the second resin. The films exhibited high levels of performance even in alkaline resistance testing using NaOH aqua solution.

However, the exact dual structure consists of two resins and its weathering resistance is unknown. Thus, the objectives of this work were (1) to verify the structure of this new blend powder coating film by using micro FTIR and (2) to determine its

resistance in artificial accelerated testing (salt water spray, heat cycle, and Xenon arc irradiation) and in outdoor exposure testing. Specifically, we wanted to confirm whether the original excellent weathering performance is maintained.

EXPERIMENTAL

Materials

Generally, there are epoxy, acryl, polyester, and hybrid (epoxy/polyester) type powder coatings. Of these, polyester coating film provides us with a relatively high thickness without pinholes and with good weathering performance, a good appearance, superior mechanical properties, and low cost.²⁴ Furthermore, polyester recycling technologies are now well established.²⁵ This provides many benefits in industrial field that meet the needs of today's society. This is why we selected the polyester type as a primary powder coating.

To improve the alkaline resistance, we mixed a primary coating resin with a secondary highly alkaline resistant resin. A thermoplastic polyester powder (SAPOE 5000, NTT-AT, Tokyo, Japan) called polyethylene terephthalate (PET) is used as the primary resin, which had a molecular weight of around 50,000, a T_m of 230–240°C, a T_g of approximately 72°C, and an average particle size of around 90 μm . In our preliminary investigations,^{21–23} we found that polyvinyl butyral (PVB) powder resin provided superior performance among the resins that we have previously tested. So, we selected PVB resin (Mowital B30H, Kuraray, Tokyo, Japan) as the secondary resin in this study, which had a molecular weight of around 25,000, a T_m of 140–170°C, a T_g of approximately 68°C, and an average particle size of around 80 μm . The samples were prepared at PET/PVB mixing ratios of 100/20, 100/25, and 100/30. We refer to these samples as PET/PVB20, PET/PVB25, and PET/PVB30, respectively.

Preparation of Blend Powder Coating Film

The coating process using the blend powder is described in a previous report.¹⁷ The base substrates were SS400 steel plates ($70 \times 150 \times 3.2 \text{ mm}^3$) that were hot-dip galvanized in accordance with JIS H8641 HDZ55²⁶ and then sweep blasted. These plates were first heated at 320°C for 20 min. Then, they were dipped in a vessel containing fluidized blend powder for 5 sec. The plates were subsequently removed and kept in air for 2 min to ensure that the powder coating materials on the plates had completely melted. The samples were then cooled by immersing them in water for 4–5 min.

Evaluation

Micro FTIR Analysis. Pieces of coating film were peeled from the steel plates, which had been coated with wax to facilitate peeling. They were cut to form a surface area and a sectional area. Each piece was observed with a digital optical microscope (VHX-900, Keyence, Tokyo, Japan), and the exact dual layer structure was analyzed with a micro FTIR (Continuum Nexus 470, Thermo Fisher Scientific, MA). This micro FTIR allowed us to obtain point analyses and profiles with a spatial resolution as high as 10 μm . Here, the different colored parts observed with the microscope were found to be around 100–300 μm in size. So we performed the analysis with a spatial resolution of 50–80 μm . Pretreatment was used to form a KBr tablet for the sectional area. The sectional area was analyzed in the transmission mode and the surface area was analyzed in the reflection mode. There were 32 and 96 scans in the transmission and reflection modes, respectively.

Color Difference and Specular Gloss. The color difference was measured with a color tester (SM-7-IS-2B, Suga Test Instruments, Tokyo, Japan) and 60° specular gloss was measured with a glossmeter (UGV-5, Suga Test Instruments, Tokyo, Japan).

Artificial Accelerated Testing

Salt Water Spray Testing. Salt water spray resistance was investigated in accordance with JISK5600-7-1.²⁷ A salt water spray instrument (STP-90V, Suga Test Instruments, Tokyo, Japan) was used in this study. Two test pieces were prepared under identical conditions, one with a cross-cut ($n = 2$). In this salt water spray testing, each test piece was observed to determine whether or not blisters, cracks, or corrosion occurred. The test period was 3500 h.

Heat Cycle Testing. Heat cycle resistance was tested using a constant temperature and humidity cryogenic unit (PL-3KPH, Espec, Osaka, Japan) to provide the accelerating environment. The temperature range was -30 to $+70^\circ\text{C}$, the relative humidity was 0–90%, and one cycle took 12 h. There were a total of 200 cycles. As with the salt water spray, after testing, the sample was checked for the occurrence of blisters, cracks, or corrosion.

Accelerated UV Testing. The UV resistance was examined in accordance with JISK5600-7-7.²⁸ A xenon arc instrument (Ci4000 Xenon Weather-Ometer, Atlas, Toyo Seiki, Tokyo, Japan) was employed. The test period was 3000 h. The pseudo solar radiation energy was 0.55 mW/mm^2 , the black panel temperature was $(63 \pm 2)^\circ\text{C}$, the chamber temperature was $(50 \pm$

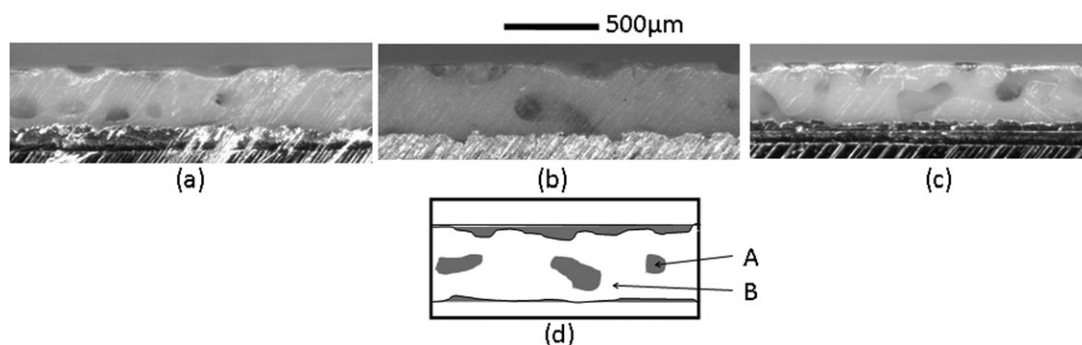


Figure 1. Images of appearance of sectional area of powder coating film. (a) PET/PVB20, (b) PET/PVB25, (c) PET/PVB30, (d) Sketch image.

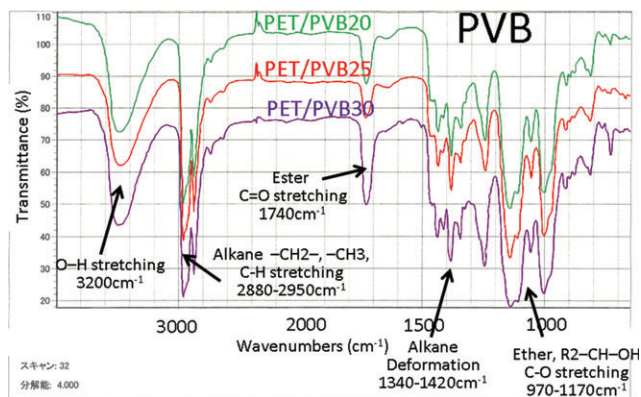


Figure 2. FTIR charts of dark part (A) in Figure 1(d). [Color figure can be viewed in the online issue, which is available at wileyonlinelibrary.com.]

10°C, the chamber relative humidity was 50%, and the water spraying time was 18 min/2 h. There were two test pieces for each test period ($n = 2$). After each test period, the color difference and the specular gloss of the coating film were measured as described above.

Outdoor Exposure Testing

The resistance to actual sunshine and an outdoor atmosphere was investigated by outdoor exposure according to JISK5600-7-6.²⁹ There were three test pieces for each condition ($n = 3$). The color difference and specular gloss were mainly tested for 8 months in the metropolitan area of Shinkiba in Tokyo to determine the influence of sunshine. The corrosion resistance was examined for 6 months in the coastal region of Miyake Island, south of Tokyo, to determine the influence of seawater particles.

RESULTS AND DISCUSSION

Structural Analysis

In previous studies,^{21–23} only the mixtures of the PET and PVB phases were identified by FTIR, and the exact structure remained unclear. Therefore, first, a distinct phase was observed with an optical microscope, then the FTIR spatial resolution

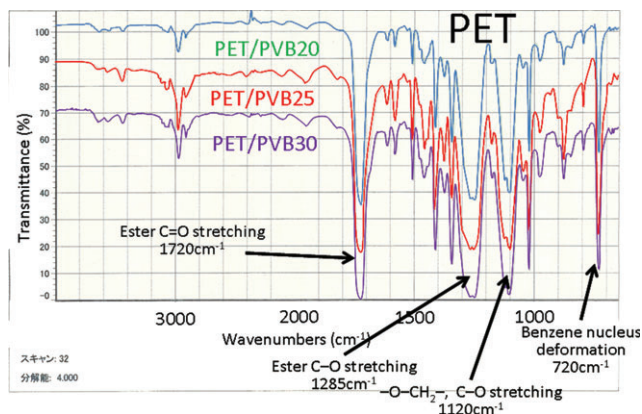


Figure 3. FTIR charts of light part (B) in Figure 1(d). [Color figure can be viewed in the online issue, which is available at wileyonlinelibrary.com.]

was confirmed to be within the size of the phase captured by the microscope. The size of the distinct phase was found to be around 100–300 μm , so we performed the analysis with a spatial resolution of 50–80 μm .

The microscope photographs are shown in Figure 1. The photographs show sectional areas of (a) PET/PVB20, (b) PET/PVB25, and (c) PET/PVB30. We can recognize two regions: a lighter region and a darker region. To make this easier to see, a sketch is provided in (d) and the regions are shown by the light and dark parts. The thickness of the dark phase in the surface layer was around 100–150 μm . The dark spot in the middle layer was around 100–300 μm [A in Figure 1(d)]. Here, we performed micro FTIR on the dark spot and light region, namely regions (A) and (B) in the sketch.

The FTIR charts we obtained are shown in Figure 2. Figure 2 shows FTIR for (A) in the sketch. From the top, they are charts of PET/PVB20, PET/PVB25, and PET/PVB30. All have a similar shape. Some characteristic absorbances were observed as follows.³⁰ The relatively sharp absorbance between 2880 and 1950 cm^{-1} was attributed to the C–H stretching of alkane $-\text{CH}_2-$

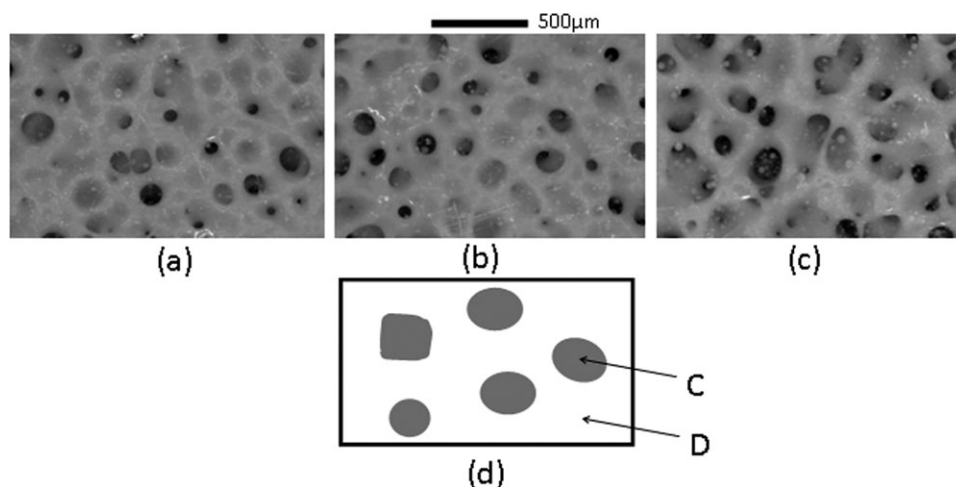


Figure 4. Images of appearance of surface area from above powder coating film. (a) PET/PVB20, (b) PET/PVB25, (c) PET/PVB30, (d) Sketch image.

and $-\text{CH}_3$ groups. The absorbance at 1740 cm^{-1} was due to $\text{C}=\text{O}$ stretching of an ester group. And, the relatively broad absorbance region between 1340 and 1440 cm^{-1} was attributed to the $\text{C}-\text{H}$ deformation of alkane $-\text{CH}_2-$ and $-\text{CH}_3$ groups. The absorbance region between 970 and 1170 cm^{-1} was due to the $\text{C}-\text{O}$ stretching of ether and secondary alcohol groups. We therefore found that these charts identify the PVB phase. We concluded that the dark region in the sectional area was only the PVB phase, and it was not mixed with the PET phase.

Figure 3 shows FTIR charts for (B) in the sketch. They all have a similar shape. Some characteristic absorbances were also observed.³⁰ The relatively sharp peak at 1720 cm^{-1} was attributed to $\text{C}=\text{O}$ stretching of an ester group. The relatively broad peaks at 1285 and 1120 cm^{-1} were due to the $\text{C}-\text{O}$ stretching of ester and $-\text{O}-\text{CH}_2-$. And, the absorbance at 720 cm^{-1} was attributed to benzene nucleus deformation. So we found that these charts identify the PET phase. Therefore, we concluded that the broad light part of the sectional area was only the PET phase.

Similarly, microscope photographs of the surface area taken from above are shown in Figure 4(a-c). It was relatively clearly observed that there were dark round spots and light parts. A sketch is shown in Figure 4(d) to make this easier to understand. The size of the round spot is approximately $100\text{--}300\text{ }\mu\text{m}$. Here, we performed micro FTIR on the spots in this dark area (C).

Figure 5 shows FTIR charts for (C) in the sketch. The characteristic sharp peaks around 3000 cm^{-1} and broad peaks between 1000 and 1300 cm^{-1} are identical to those in Figure 2, which indicates the PVB phase. These phenomena confirmed that PVB formed a distinct domain with a size of around $100\text{--}300\text{ }\mu\text{m}$. That is, this secondary PVB resin provides an individual domain. We also show FTIR charts for (D) in the sketch, which is the light region, in Figure 6. Surprisingly, all the peaks were exactly the same as those for (C). We identified both the (C) and (D) regions as the PVB phase.

It is known that the rule of mixtures generally does not hold in polymer blends because the blend components are not usually miscible and form a two-phase structure.³¹ Therefore, the possible formation process is considered to be as follows along with Figure

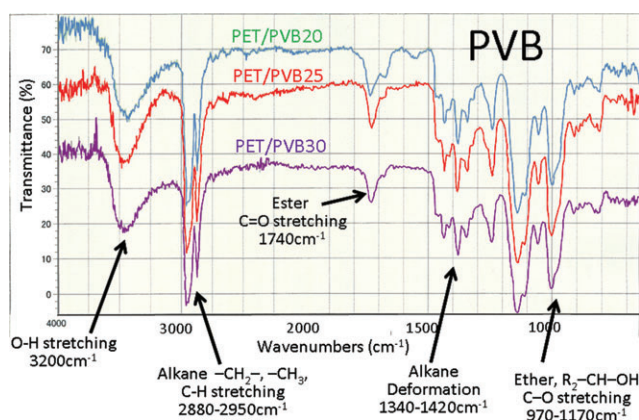


Figure 5. FTIR charts of dark part (C) in Figure 4(d). [Color figure can be viewed in the online issue, which is available at wileyonlinelibrary.com.]

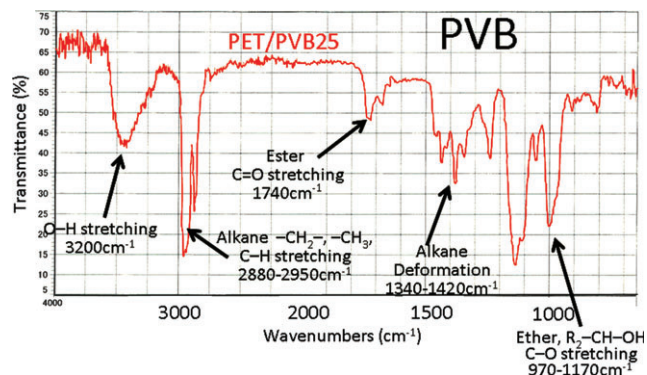


Figure 6. FTIR charts of light part (D) in Figure 4(d). [Color figure can be viewed in the online issue, which is available at wileyonlinelibrary.com.]

7. First, the mixed powder coating of PET and PVB was heated above their T_m s so that both components were melted (1 in Figure 7). Second, the temperature decreased during quenching. PET, which has the higher T_m , precipitated earlier than PVB to form the coat (2 in Figure 7). Consequently, the PVB remained in position or was pushed toward the upper side and lower side (3 in Figure 7). Finally, the PVB coagulated to form a continuous layer on the surface layer (4 in Figure 7). In contrast, a PVB spot remained in the middle layer and formed a spot domain structure.

In this investigation, Figures 1 and 2 demonstrate that the surface area, which is dominated by a dark phase, consisted entirely of the PVB phase. So, both (C) and (D) seen from above were only the PVB phase. We attribute the color difference between (C) and (D) to the difference in the thickness of each phase. The details are being investigated. We found that many PVB domains accumulate and connect to form a continuous phase in the surface layer. We expect this continuous PVB phase to protect the film against the outdoor environment. The next section describes the weathering resistance.

Indoor Accelerated Weathering Resistance

Salt Water Spray Resistance. Salt water spray resistance was investigated in accordance with JISK5600-7-1.²⁵ Figure 8 shows the PET/PVB20, PET/PVB25, and PET/PVB30 test pieces after 3500 h of spray testing. No blisters, cracks, or peeling was observed for any of the pieces. Of course, the cross-cut part

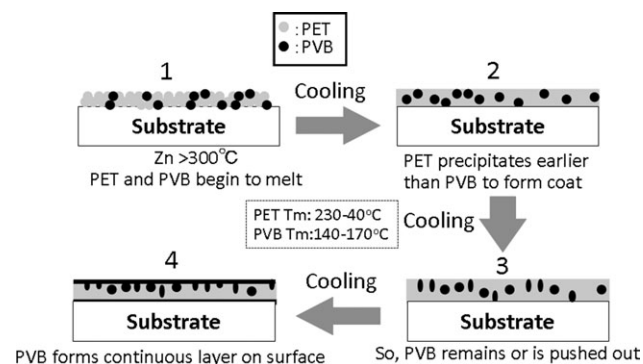


Figure 7. Possible structure formation process.

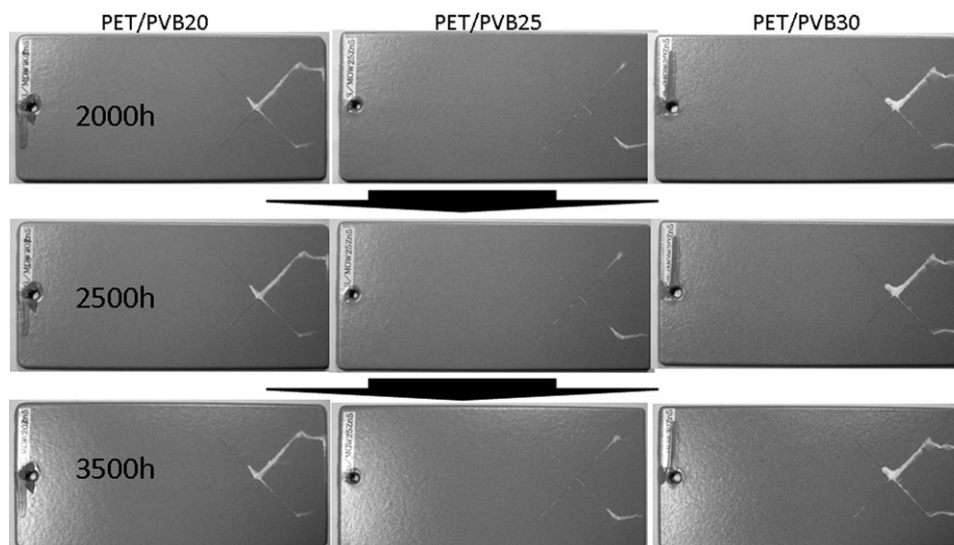


Figure 8. Test pieces after salt water spray testing.

contained small particles of white rust, but this did not develop after 2000 h. There was no blistering or peeling surrounding the cross-cut. Therefore, we found that the dual layer structural thermoplastic polyester powder coating film offers good anti-corrosion performance even when exposed to salt water spray for 3500 h.

Heat Cycle Resistance. Heat cycle resistance was tested in a constant temperature and humidity cryogenic unit from -30 to $+70^{\circ}\text{C}$. Figure 9 shows the test pieces after 200 cycles. There appears to be no white rust, blistering, cracking, or peeling in the images. However, one or two small blisters were observed on the coating. The reason for this is now being considered, but perhaps the air remaining in the Zn steel was expelled at $+70^{\circ}\text{C}$ because the temperature rose above the T_g of the secondary powder coating film (68°C). And, air would cause blistering relatively easily.

UV Resistance. The UV resistance was examined in accordance with JISK5600-7-7.²⁸ Figure 10 shows the test pieces after 2500 h. And the color difference and specular gloss are shown in Figures 11 and 12, respectively. In Figure 10, PET/PVB20, PET/PVB25, and PET/PVB30 all have the same appearance. Figure 11 shows the color difference quantitatively, and it increased with the testing time. The plot is the average of two measurements for each time. When the PVB mixing ratio increased, the degree of color change decreased. So it is considered that the secondary PVB layer contributes to protecting the film against

color changes caused by UV light. In contrast, the specular gloss in Figure 12 decreased with the testing time when the PVB mixing ratio increased. This is probably because the PVB itself is degraded by the UV light and this causes surface roughness that could degrade the specular gloss. We therefore checked the surface roughness by employing a surface texture measuring instrument (Surfcom570A, ACCRETECH, Tokyo, Japan). It revealed that the surface roughness R_{max} at 3000 h is 136.7, 142.2, and $167.4\ \mu\text{m}$ for PET/PVB20, PET/PVB25, and PET/PVB30, respectively. These data were in agreement with the above consideration.

Outdoor Exposure Resistance

Finally, we performed outdoor exposure testing at a metropolitan site (Shinkiba in Tokyo), and at a coastal site (Miyake Island), in accordance with JISK5600-7-6.²⁹ The former experiment was designed to determine the weathering resistance; the color difference; and the specular gloss under sunshine. The latter experiment was undertaken to observe the corrosion resistance to a high density of seawater particles.

The color difference and the specular gloss are shown in Figures 13 and 14, respectively ($n = 3$). Figure 13 shows the color difference for PET/PVB25 and only PET. The color difference increased gradually with exposure time, and the degree of increase was large when the PVB content was high. During outdoor exposure, we can consider that dust in the atmosphere could affect the surface of the coating resulting in a large color

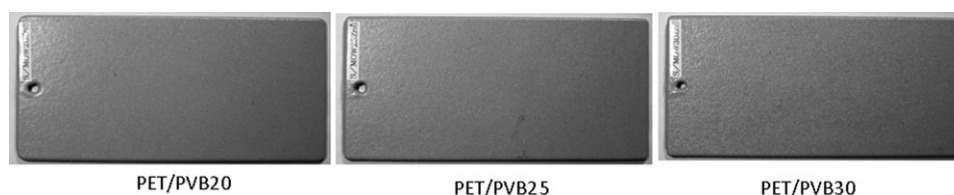


Figure 9. Test pieces after 200 cycles of heat cycling testing.

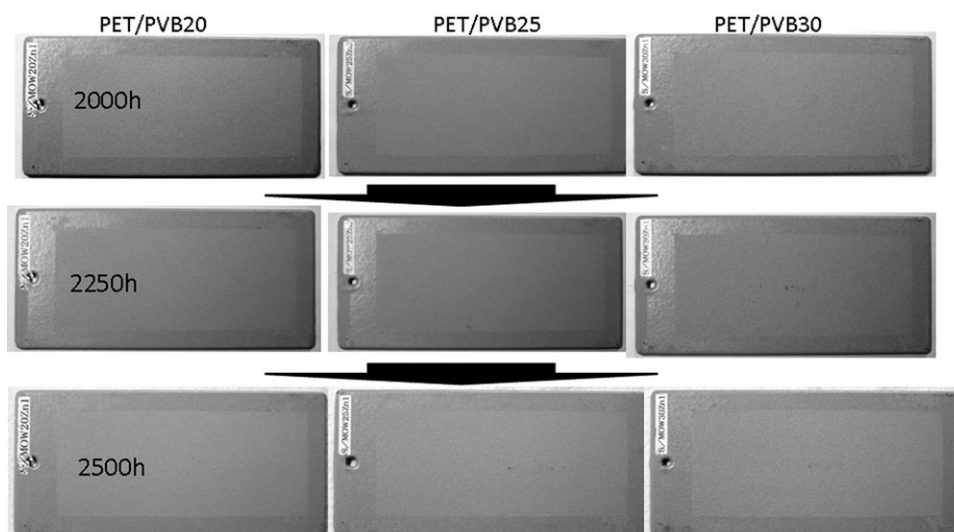


Figure 10. Test pieces after UV testing.

difference, apart from the PVB preventing the color change. An interesting point was the difference in the increase seen in Figures 11 and 13. In the indoor UV testing, the degree of color difference seems to saturate. In contrast, in outdoor exposure it seems to continue increasing. This may be because the color change is caused by a different mechanism. The details are being investigated.

Figure 14 shows the specular gloss for PET/PVB25 and for PET alone. In both cases the specular gloss decreased with the exposure time. When the PVB content was high, the decrease was large. That is, the presence of PVB resulted in inferior weathering performance in terms of specular gloss. This is the same as in Figure 12. It was also interesting to note that the trend was completely different from that in Figure 12. Figure 14 shows only a 30–40% decrease, while Figure 12 shows a decrease of over 90%. This difference is also in agreement with our previous studies.¹⁷ The reason may be a difference between the specular gloss degradation mechanisms in the accelerated testing and outdoor exposure. The details are now being investigated.

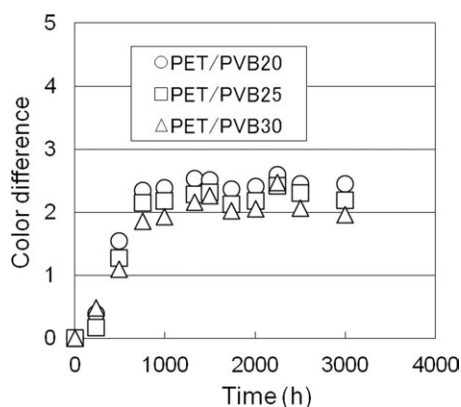


Figure 11. Color difference in indoor UV testing.

The surface appearance after 8 months exposure in Shinkiba is shown in Figure 15. In Figure 15 there is no blistering, cracking, peeling, or white rust, even around the cross-cut part. Therefore, the weathering resistance was maintained. The surface appearance after 6 months exposure in Miyake Island is shown in Figure 16.

In Figure 16, there is no blistering, cracking, peeling, or white rust even close to the cross-cut part. From these observations, we found that the salt water particle resistance was sufficient for up to 6 months at the coastal area site on Miyake Island.

CONCLUSIONS

To verify the exact structure of a new blend of thermoplastic powder coating film, micro FTIR analysis was performed to the point with a high spatial resolution. And, resistance to certain artificial accelerated conditions and actual outdoor exposure conditions were examined to confirm the performance as a protective coating for use in the telecommunication field. Our findings were as follows:

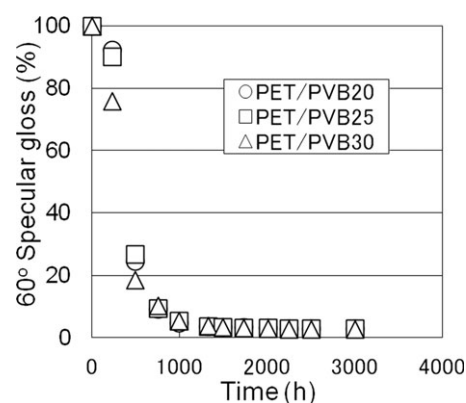


Figure 12. Specular gloss in indoor UV testing.

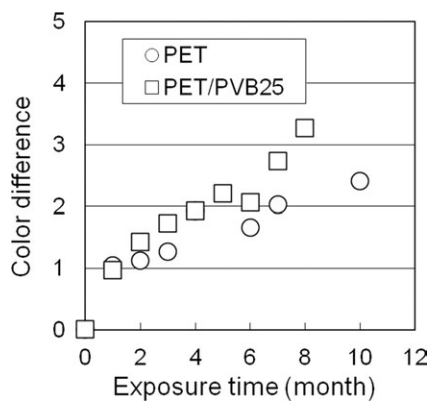


Figure 13. Color difference in outdoor exposure in Shinkiba.

Our new blend powder coating film has a distinct dual phase structure consisting of primary PET and secondary PVB resins. In our observation of a sectional area, the secondary PVB resin provided domains with sizes of 100–300 μm . Specifically, the PVB domains accumulated and connected to form a continuous phase in the surface layer whose thickness was approximately 100–150 μm . The PVB in the middle layer exhibited a distinct round domain with a size of around 100–300 μm .

Even in salt water spray testing, the dual phase structure film did not blister, crack, peel, or develop white rust during the investigation period. A small amount of white rust was observed immediately around the cross-cut; however, we confirmed that this did not expand. We concluded that even when the PET powder coating contains the secondary PVB powder the salt water resistance is maintained for 3500 h.

In accelerated UV testing, the color difference performance was improved by including PVB. However, the specular gloss performance was not as good as that of the original film. We considered that the PVB itself could be sacrificed to maintain a good color difference; however the consequent high surface roughness would degrade the specular gloss.

In actual outdoor exposure at a site in a metropolitan area (Shinkiba, Tokyo) and a coastal area (Miyake Island), the color difference and specular gloss showed a similar trend in indoor weathering tests, but there was a difference in their absolute val-

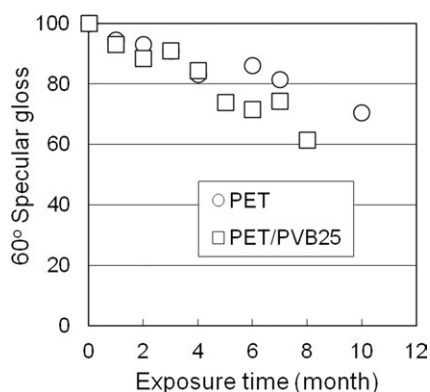


Figure 14. Specular gloss in outdoor exposure in Shinkiba.

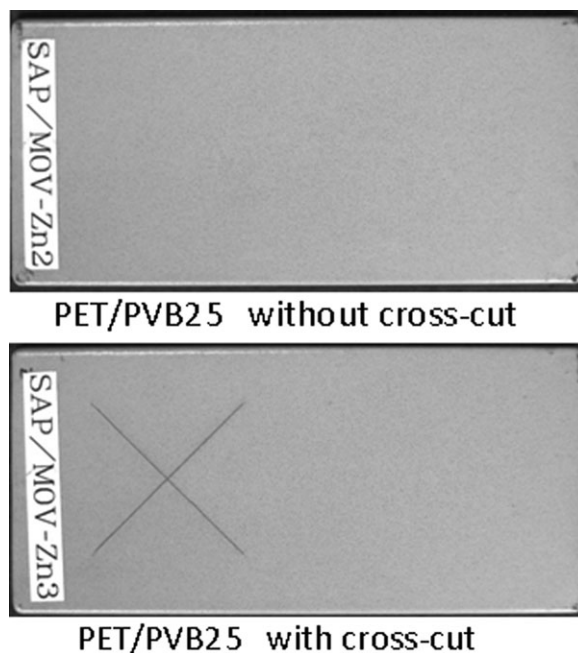


Figure 15. Surface appearance of PET/PVB25 after 8 months exposure in Shinkiba.

ues, which was probably caused by their different mechanisms. Finally, the surface appearance after outdoor exposure of up to 6 and 8 months, respectively, remained good. We found that the dual phase structural powder coating maintained the original excellent weathering performance throughout the study period.

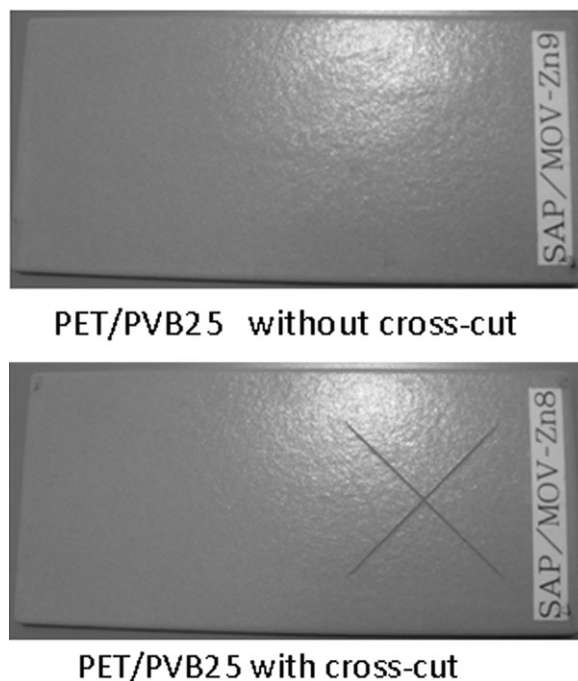


Figure 16. Surface appearance of PET/PVB25 after 6 months exposure in Miyake Island.

ACKNOWLEDGMENTS

The authors are grateful to Prof. Griffiths at the University of Idaho for his lecture on FTIR analysis and helpful discussions, and to the members of the Technical Support Center at NTT East for providing the exposure site on Miyake Island.

REFERENCES

1. Sawada, T.; Takeshita, Y.; Saito, H.; Higashi, Y.; Sakata, S.; Handa, T. *NTT Tech. Rev.* **2009**, *8*, 10; <https://www.ntt-review.jp/archive/ntttechnical.php?contents=ntr200910sf4.html> (accessed April 9, 2012).
2. Sawada, T.; Saito, H.; Higashi, Y.; Sakaino, H. *NTT Tech. Rev.* **2009**, *9*, 2; <https://www.ntt-review.jp/archive/ntttechnical.php?contents=ntr201102fa6.html> (accessed April 9, 2012).
3. Saito, H. 2008 Reports on Weathering Technology Achievements; Japan Weathering Test Center: Tokyo, **2008**; p 75.
4. Nakamura, M.; Saito, H.; Higashi, Y.; Sawada, T.; Handa, T.; Kudo, T.; Watanabe, M.; Matsumoto, M. *Zairyo-to-Kankyo* **2010**, *59*, 377.
5. Saito, H.; Sawada, T.; Handa, T. *J. Mater. Test. Res. Assoc. Jpn.* **2010**, *55*, 109.
6. Miyata, Y.; Takekoshi, R.; Takazawa, H. *Corros. Eng.* **1989**, *38*, 540.
7. Takeshita, Y. 2010 Reports on Weathering Technology Achievements; Japan Weathering Test Center: Tokyo, **2010**; p 25.
8. Takeshita, Y.; Sakata, S.; Sawada, T.; Jackson, R., Jr.; Nishio, R. In Pacificchem 2010, paper ID.23, Honolulu, Hawaii, Dec 15–21, 2010; The International Chemical Congress of Pacific Basin Societies, **2010**.
9. Takeshita, Y.; Sakata, S.; Sawada, T.; Jackson, R. A., Jr.; Nishio, R. *Zairyo-to-Kankyo* **2011**, *60*, 147.
10. Takeshita, Y.; Jackson, R. A.; Sakata, S.; Sawada, T.; Nishio, R. *Polym. Eng. Sci.* **2012**, *52*, 572.
11. Kamisho, T.; Takeshita, Y.; Sakata, S.; Sawada, T. In 31st Bosei Boshoku Gijyutyu Happyo Taikai Koen Yokoshu, Tokyo, Japan, July 7–8, 2011; JACC: Tokyo, **2011**.
12. Kamisho, T.; Takeshita, Y.; Sakata, S.; Sawada, T. *Bosei-Kanri* **2011**, *55*, 449.
13. Takazawa, H. In CORROSION91, paper no. 484, Cincinnati, OH; NACE, **1991**.
14. Handa, T.; Takazawa, H. In CORROSION98, paper no. 516, Houston, TX; NACE, **1998**.
15. Takeshita, Y.; Handa, T.; Kudo, T. In APCCC15, paper no. CS-02, p.142, Manila, Philippines, Oct 18–21, 2009; PhiCS, **2009**.
16. Nishio, R.; Watanuki, Y.; Takeshita, Y.; Handa, T. In 29th Bosei Boshoku Gijyutyu Happyo Taikai Koen Yokoshu, Tokyo, Japan, July 9–10, 2009; JACC: Tokyo, **2009**.
17. Takeshita, Y.; Handa, T.; Kudo, T. *Zairyo-to-Kankyo* **2010**, *59*, 228.
18. Watanuki, Y.; Kudo, T.; Takeshita, Y.; Sawada, T.; Handa, T. In 30th Bosei Boshoku Gijyutyu Happyo Taikai Koen Yokoshu, Tokyo, Japan, July 8–9, 2010; JACC: Tokyo, **2010**.
19. Takeshita, Y.; Sawada, T.; Handa, T.; Kudo, T. In CORROSION2011, paper no.11374, Houston, TX, March 13–17, 2011; NACE, **2011**.
20. Hare, C. H. In Paint Film Degradation Mechanisms and Control; Brady, R. F., Jr., Ed.; SSPC: Pittsburgh, PA, **2001**; Chapter 20, p 155.
21. Takeshita, Y.; Kamisho, T.; Sakata, S.; Sawada, T.; Watanuki, Y.; Ueda, T. In 18th International Corrosion Congress, paper no. 60, Perth, Australia, Nov 20–24, 2011; ICC, **2011**.
22. Watanuki, Y.; Ueda, T.; Nishio, R.; Takeshita, Y.; Sawada, T. In 31st Bosei Boshoku Gijyutyu Happyo Taikai Koen Yokoshu, Tokyo, Japan, July 7–8, 2011; JACC: Tokyo, **2011**.
23. Watanuki, Y.; Ueda, T.; Nishio, R.; Takeshita, Y.; Sawada, T. *Bosei-Kanri* **2012**, *56*, 24.
24. Onishi, K. Development and Prospect of Powder Coating, CMC: Tokyo, Japan, **2006**; p 8.
25. Kawamura, C.; Ito, K.; Nishida, R.; Yoshihara, I. *Prog. Org. Coat.* **2002**, *45*, 185.
26. JIS H 8641, “Hot dip galvanized coatings”, Tokyo, Japan, **2007**, (ISO 1461:1999).
27. JIS K 5600-7-1, “Testing methods for paints—Part 7: Long-period performance of film—Section 1: Resistance to neutral spray”, Tokyo, Japan, **1999**, (ISO 7253:1984).
28. JIS K 5600-7-7, “Testing methods for paints—Part 7: Long-period performance of film—Section 7: Accelerated weathering (Exposure to filtered xenon-arc radiation)”, Tokyo, Japan, **1999**, (ISO 11341:1994).
29. JIS K 5600-7-6, “Testing methods for paints—Part 7: Long-period performance of film—Section 6: Natural weathering”, Tokyo, Japan, **2002**.
30. Japan Paint Inspecting Association. Handbook of FT-IR Spectrums of Coating Resin, Tokyo, Japan, **1975**; p 11, p 56.
31. Lashgari, S.; Azar, A. A.; Lashgari, S.; Gezaz, S. M. *J. Vinyl Addit. Technol.* **2010**, *16*, 246.